JACS
JOURNAL OF THE AMERICAN CHEMICAL SOCIETY
Communication
pubs.acs.org/JACS

Protonation-Induced Chromism of Pyridylethynyl-Appended [core+*exo*]-Type Au_8 Clusters. Resonance-Coupled Electronic Perturbation through π-Conjugated Group

Naoki Kobayashi,[†] Yutaro Kamei,[†] Yukatsu Shichibu,[†,‡] and Katsuaki Konishi*[,†,‡]

[†]Graduate School of Environmental Science, Hokkaido University, North 10 West 5, Sapporo 060-0810, Japan
[‡]Faculty of Environmental Earth Science, Hokkaido University, North 10 West 5, Sapporo 060-0810, Japan

Supporting Information

ABSTRACT: A series of [core+*exo*]-type Au_8 clusters bearing two alkynyl ligands on the *exo* gold atoms ($[Au_8(dppp)_4(C{\equiv}CR)_2]^{2+}$, **2**–**6**) were synthesized by the reaction of $[Au_8(dppp)_4]^{2+}$ (**1**) with alkynyl anions. Although the C≡C moieties directly attached to the Au_8 units did not affect the optical properties arising from intracluster transitions, the pyridylethynyl-bearing clusters (**4**–**6**) exhibited reversible visible absorption and photoluminescence responses to protonation/deprotonation events of the terminal pyridyl moieties. The chromism behaviors and proton-binding constants of these clusters were highly dependent on the relative position of the pyridine nitrogen atom, such that the 2-pyridyl (**4**) and 4-pyridyl (**6**) isomers showed more pronounced responses than the 3-pyridyl isomer (**5**). These results suggest that the resonance-coupled movement of the positive charge upon protonation is involved in the optical responses, where the formation of extended charged resonance structures causes significant perturbation effects on the electronic properties of the Au_8 unit and also contributes to the high binding affinities.

The interaction between gold and C≡C π systems continues to be of interest because it has a number of versatile applications.[1−9] Simple complexes of gold(I) and gold(III) have been extensively studied with regard to their unique photoluminescence (PL)[2,6−12] as well as their crucial role in some catalytic organic reactions.[13−15] However, although phosphine- and thiolate-capped gold clusters and nanoparticles have been well characterized,[16−20] examples of alkyne (alkynyl)-modified clusters/nanoparticles are quite rare[21,22] and so the potential interactions between C≡C π systems and a gold kernel have been left unexplored. Herein we report the first phosphine-coordinated molecular gold clusters having alkynyl substituents (**2**–**6**). We also show the acid-induced chromism of pyridylethynyl-modified clusters (**4**–**6**), in which the resonance structures of the protonated π-conjugated systems play a vital role in affecting the optical properties of the Au_8 cluster.

The attachment of alkynyl groups onto Au_8 clusters was accomplished via the reaction of divalent Au_8 cluster cations ($[Au_8(dppp)_4]^{2+}$, **1**)[23] with terminal alkynes (RC≡CH) under basic conditions (Scheme 1). In a typical reaction, a methanol solution of **1**·$(NO_3)_2$ was treated with phenylacetylene (2 molar equiv) in the presence of sodium methoxide (300 equiv) and the mixture was stirred at room temperature. After 10 h, the ESI-MS spectrum of the reaction mixture was primarily dominated by a set of signals appearing at m/z ∼1714 due to the formation of the product $[Au_8(dppp)_4(C{\equiv}CC_6H_5)_2]^{2+}$ (**2**), while the signals at m/z ∼1613 due to $[Au_8(dppp)_4]^{2+}$ (**1**), which had been observed as the sole cluster species before the reaction, had completely disappeared. Signals due to other cluster species were observed only at negligible intensities, indicating that **1** was converted almost exclusively to **2**. The reactions of **1** with other aryl- and alkyl-alkynes also proceeded smoothly to afford the dialkynylated clusters (**3**–**6**) (Scheme 1), each of which exhibited strong ESI-MS signals assignable to the expected $[Au_8(dppp)_4(C{\equiv}CR)_2]^{2+}$ species (Figure S1).

Scheme 1. Dialkynylation of Au_8 Cluster

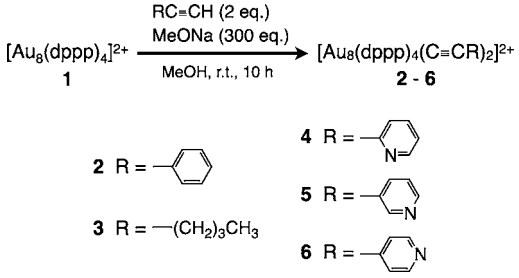

Although **1**–**6** are all divalent, the Au_8 moieties in **1** and **2**–**6** had differing charges of 2+ and 4+, respectively. Single-crystal X-ray structural analyses of **1** and **2** revealed that they had different octagold geometric structures, as shown in Figure 1. Product **2** had a bitetrahedral Au_6 core in addition to two *exo* gold atoms extending outward at opposite edges of the bitetrahedron (Figure 1b), while **1** adopted an edge-shared tritetrahedral geometry (Figure 1a).[23] These structures indicate that the nucleophilic attack of the alkynyl anion may facilitate the two-electron oxidation of the tritetrahedral octagold framework of **1**, allowing rearrangement of the cluster to the [core+two]-type geometry and selective introduction of two alkynyl groups at the two *exo* gold atoms.

The structure of **2** shows that each of the two *exo* gold atoms accommodates one phosphine and one alkynyl group, such that

Received: September 25, 2013
Published: October 15, 2013

   dx.doi.org/10.1021/ja4099092 | *J. Am. Chem. Soc.* 2013, 135, 16078−16081

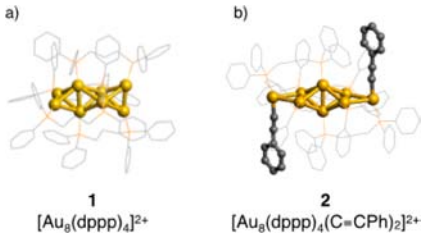

Figure 1. Crystal structures of cationic moieties of (a) **1** and (b) **2** with hydrogen atoms omitted for clarity.

the two C≡C bonds are *trans*-oriented and directed into positions which are almost perpendicular to the *exo*-containing triangles. The molecular structure of **2** in the solid state appears to be retained in solution; the ^{31}P NMR spectrum of **2**·$(NO_3)_2$ in CD_3OD showed signals at 38.8, 51.4, and 55.6 ppm with an integrated intensity ratio of 1:2:1 (Figure S2a), which is consistent with the results expected from the crystal structure. The ^{31}P NMR spectra of products **3**–**6** were similar to that of **2** (Figure S2), indicating that they have analogous structures based on a [core+*exo*]-type (Au_6+2Au) geometry.

These dialkynylated clusters (**2**–**6**) all exhibited an isolated absorption band in the visible region of the spectrum. This result is similar to that reported for the isostructural dichloro-substituted cluster ($[Au_8(dppp)_4Cl_2]^{2+}$, **7**), which has been synthesized by a different route involving the reaction of $[Au_6(dppp)_4]^{2+}$ with $Au(PPh_3)Cl$.[23] In a previous study concerning the electronic structure of [core+*exo*]-type clusters, including **7**, we demonstrated that the visible absorption band results from an electronic transition within the Au_8 moiety.[24,25] Thus, if the C≡C π-electrons of **2**–**6** undergo significant interactions with the electrons of the cluster unit, noticeable band shifts would be expected. The absorption band positions of these species (Figure 2a, blue lines), however, were almost identical to that of dichloro-type cluster **7** (λ_{max} = 510 ± 2 nm).[23] Therefore, it is likely that the Au_8 cluster units of **2**–**6** are electronically separated from the directly attached conjugated systems. Furthermore, the photoluminescence properties of the alkynylated clusters (**2**–**6**) were also similar

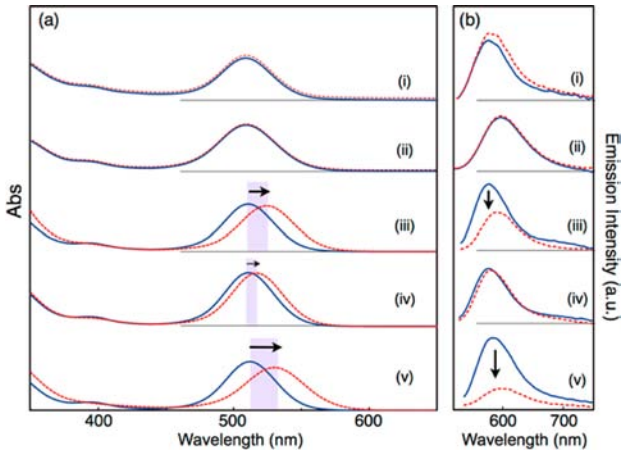

Figure 2. Absorption (a) and photoluminescence (b) spectra of **2** (i, λ_{ex} = 509 nm), **3** (ii, λ_{ex} = 509 nm), **4** (iii, λ_{ex} = 518 nm), **5** (iv, λ_{ex} = 515 nm), and **6** (v, λ_{ex} = 523 nm) in MeOH (10 μM) at 25 °C before (blue solid lines) and after (red dotted lines) the addition of HCl (370 molar equiv). The excitation wavelengths were chosen so as to have the same absorbance before and after the HCl addition.

to that of **7**,[23] exhibiting bands at ~580 nm upon excitation of the visible bands (~510 nm) (Figure 2b, blue lines). The excitation spectra were almost exactly superimposed with the absorption spectra, indicating that the luminescence bands are associated with intracluster transitions.

As noted above, the attachment of π-conjugated organic moieties to the Au_8 cluster appears to have little effect on the cluster's electronic properties. We did, however, find that the pyridylethynyl-type clusters exhibited definite optical responses subsequent to protonation. For example, when the 4-pyridylethynyl-substituted cluster (**6**) was dissolved in methanol (10 μM, 3 mL) and mixed with hydrochloric acid (370 molar equiv), the absorption band shifted from 512 to 531 nm (Figure 2a (v), Table 1 (entry 5)) and the color of the solution

Table 1. HCl-Induced Absorption Spectral Changes of 2–6 and the Association Constants for Monoprotonation of the Free Base Forms

entry	cluster	R	λ_f[a]	λ_c[b]	$\Delta\lambda$ (nm)	K_1 (M^{-1})[c]
1	**2**	Ph	509	509	0	–
2	**3**	*n*-Bu	509	509	0	–
3	**4**	2-Py	511	524	13	5.9×10^3
4	**5**	3-Py	511	517	6	1.3×10^3
5	**6**	4-Py	512	531	19	1.2×10^4

[a]λ_{max} of the free base form in MeOH (10 μM). [b]λ_{max} in the presence of HCl (3.7 mM). [c]Estimated from the titration profiles by a nonlinear curve fitting method (see Supporting Information).

transitioned from light pink to deep pink. Spectrophotometric titration experiments (Figure S4c) showed that plots of the absorbance at 543 nm versus $[HCl]_0/[\mathbf{6}]_0$ increased continuously until plateauing at a molar ratio of ~200 (Figure 3).

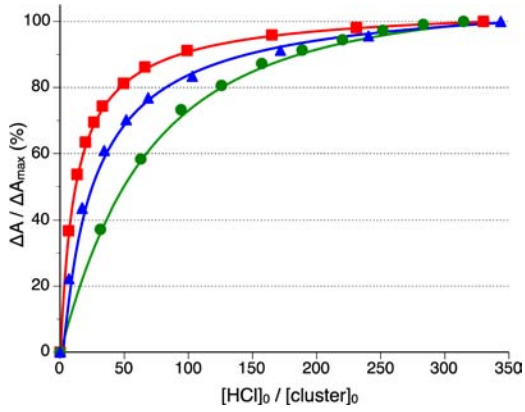

Figure 3. Spectrophotometric titration of **4** (▲, 9.7 μM), **5** (●, 10.6 μM), and **6** (■, 10.1 μM) in MeOH with aqueous HCl at 25 °C. Monitoring wavelengths: 537, 533, and 543 nm for **4**, **5**, and **6**, respectively. The curves are drawn to fit a 1:2 host–guest binding system.

Similar spectral change and binding profiles were observed when **6** was titrated with other protonic acids such as $MeSO_3H$ and HBF_4 (Figure S5). These results indicate that protonation of the pyridyl moiety rather than interaction with the counterion (such as Cl^- or $MeSO_3^-$) is likely the primary cause of the spectral change. In fact, unfunctionalized clusters (**2** and **3**) showed negligible spectral responses under similar conditions (Figure 2a (i, ii), Table 1 (entries 1 and 2)). Thus, the formation of a cationic charge at the distal pyridyl nitrogen

dx.doi.org/10.1021/ja4099092 | J. Am. Chem. Soc. 2013, 135, 16078–16081

has been shown to significantly affect the electronic properties of the Au_8 moieties.

The other pyridylethynyl-modified clusters (**4** and **5**) also showed definite acid-induced red shifts of the absorption band (Figure 2a), although the extent of the optical responses notably varied with the nitrogen position of the pyridine functionality. As a result, the red shift ($\Delta\lambda$) of the 3-pyridyl isomer (**5**) upon mixing with 370 equiv of HCl was only 6 nm (511 → 517 nm) (iv), which is significantly less than the shifts observed for the 4-pyridyl (**6**, $\Delta\lambda$ = 19 nm) (v) and 2-pyridyl (**4**, $\Delta\lambda$ = 13 nm) (iii) isomers. The binding isotherms of the three regioisomers upon titration with HCl were also different from one another (Figure 3). The association constants for the initial protonation (K_1) of each free-base cluster were estimated using a nonlinear least-squares fit[26] to be 5.9×10^3, 1.3×10^3, and 1.2×10^4 M^{-1} for **4**, **5**, and **6**, respectively (Table 1, entries 3−5). These data demonstrate that not only the band shifts ($\Delta\lambda$) but also the proton-binding activities (K_1) are affected by the relative position of the nitrogen atom in the pyridine functionality.

The observed differences in the optical responses of the 2-/4-pyridyl isomers (**4** and **6**) and the 3-pyridyl isomer (**5**) suggest that resonance structures of the protonated pyridylethynyl group are involved in the spectral shifts. As shown in Figure 4a,

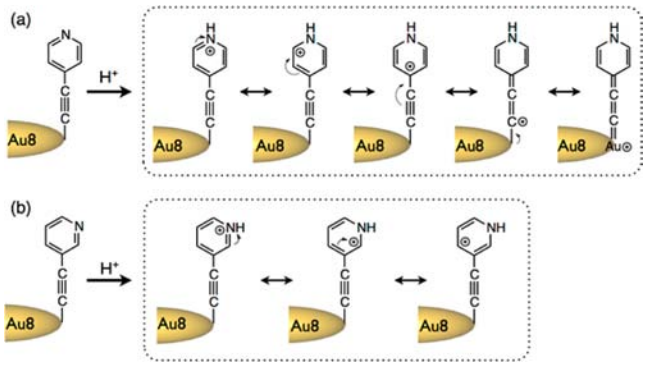

Figure 4. Plausible resonance contributors of (a) **6** and (b) **5** upon protonation.

when the 4-pyridylethynyl group in **6** is protonated, the positive charge can move not only within the aromatic ring but also to the C≡C unit to give a resonance contributor with the positive charge on the carbon atom adjacent to the *exo* gold atom. The positive charge at this location may affect the electronic structure of the proximal Au_8 cluster unit, inducing a significant shift of the absorption band. Furthermore, as shown in the figure, the formation of a gold−allenylidene species may be possible upon back-donation of electron density from the Au_8 moiety,[12,27] which should result in an even more direct perturbation effect on the cluster's electronic structure. Similar resonance contributors can be expected to exist in the protonated form of **4**. In contrast, the same extended resonance structure would not be possible in the case of the protonated form of **5**, since the location of the positive charge is limited solely within the pyridine ring (Figure 4b). Consequently, the positive charge, which is gained by protonation, has only a minor effect on the cluster's electronic properties and thus leads to a small protonation-induced shift.

As we have seen, the acid-induced changes in the absorption spectral responses of **4**−**6** can be correlated with the resonance structures of their protonated forms. The involvement of such resonance structures is further supported by the affinities of **4**−**6** for protonic acids. Thus, the protonated forms of **4** and **6** should be more thermodynamically stable than that of **5**, based on consideration of the varieties of possible resonance contributors in the 4- and 2-pyridyl isomers. This trend was indeed clearly observed in the titration profiles (Figure 3) and in the values of the binding constants (Table 1), which show the higher proton-binding affinities of **4** and **6** compared to **5**.

Resonance-coupled perturbation effects of the distal protonation events were also evident in the photoluminescence response of **6**. A notable decrease (∼80%) in the emission intensity of **6** was observed upon mixing with HCl (Figure 2b (v)), whereas no quenching was observed in the case of the 3-pyridyl isomer (**5**, Figure 2b (iv)). Therefore, it is probable that the excited state of the Au_8 moiety is efficiently quenched when a positive charge is located either within the cluster or close to the cluster (Figure 4a), whereas a positive charge on the distal pyridine ring produces a much less pronounced quenching effect. It should be noted that the emission of the 2-pyridyl isomer (**4**) was not significantly quenched (Figure 2b (iii)), perhaps due to the specific resonance contributor. It is possible that a contributing resonance structure having the cationic charge at the *ipso* carbon (**4′**), which should be especially stabilized by the adjacent nitrogen lone pair,[27,28] hampers subsequent transfer of the charge to the C≡C and Au_8 cluster moieties.

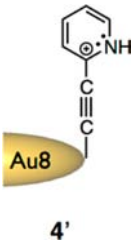

4′

Finally, we would like to note that the absorption and PL changes of the pyridylethynyl-modified clusters were found to be completely reversible. As an example, the spectrum of the protonated form of **6** reverted to its original pattern upon neutralization of the solution by the addition of a base such as 2-ethanolamine (Figure S6). Furthermore, these reversible spectral and color depth changes were stable and fully reproducible throughout repeated cycles of acidification and neutralization. This reversible response was also observed in aqueous solvent (95% water), indicating that this system has the potential to act as a pH indicator.

In conclusion, we have demonstrated the synthesis of phosphine-protected clusters having dialkynyl substituents and the unique protonation-responsive chromism of pyridylethynyl-substituted clusters. Through the chromism behaviors, we provide an example of the resonance-coupled transmission of chemical information to a distal cluster unit through π-conjugated groups. The possibility of tailoring the design of the π-conjugated pendant ligands is worthy of further investigation with regard to the development of cluster-based functional modules.

■ ASSOCIATED CONTENT

Ⓢ Supporting Information

Details of syntheses and spectral characterization data of **2**−**6**, crystal data (cif file) of **2**, and determination of association

dx.doi.org/10.1021/ja4099092 | J. Am. Chem. Soc. 2013, 135, 16078−16081

constants as well as supporting Figures S1−S6. This material is available free of charge via the Internet at http://pubs.acs.org.

AUTHOR INFORMATION

Corresponding Author

konishi@ees.hokudai.ac.jp

Notes

The authors declare no competing financial interest.

ACKNOWLEDGMENTS

This work was partially supported by the MEXT/JSPS Grant-in-Aids (20111009 (Innovative Areas "Emergence in Chemistry") for K.K. and 24750001 for Y.S.), the Asahi Glass Foundation (K.K.), and the Sasakawa Scientific Research Grant and Tanaka Precious Metals Group (Y.S.). We also thank Japan Science and Technology Agency (JST), Advanced Low Carbon Technology Research and Development Program (ALCA) for support to K.K.

REFERENCES

(1) Long, N.; Williams, C. *Angew. Chem., Int. Ed.* **2003**, *42*, 2586−2617.
(2) Lima, J.; Rodríguez, L. *Chem. Soc. Rev.* **2011**, *40*, 5442−5456.
(3) Hashmi, A. *Chem. Rev.* **2007**, *107*, 3180−3211.
(4) Gorin, D.; Toste, F. *Nature* **2007**, *446*, 395−403.
(5) Braun, I.; Asiri, A. M.; Hashmi, A. S. K. *ACS Catal.* **2013**, *3*, 1902−1907.
(6) López de Luzuriaga, J. M. Luminescence of Supramolecular Gold Containing Materials. In *Modern Supramolecular Gold Chemistry: Gold-Metal Interactions and Applications*; Wiley-VCH: Weinheim, 2008; pp 347−401.
(7) Yam, V.; Cheng, E. *Chem. Soc. Rev.* **2008**, *37*, 1806−1813.
(8) Bronner, C.; Wenger, O. *Dalton Trans.* **2011**, *40*, 12409−12420.
(9) He, X.; Yam, V. W.-W. *Coord. Chem. Rev.* **2011**, *255*, 2111−2123.
(10) Au, V.; Wong, K.; Tsang, D.; Chan, M.-Y.; Zhu, N.; Yam, V. *J. Am. Chem. Soc.* **2010**, *132*, 14273−14278.
(11) Koshevoy, I.; Chang, Y.-C.; Karttunen, A.; Selivanov, S.; Jänis, J.; Haukka, M.; Pakkanen, T.; Tunik, S.; Chou, P.-T. *Inorg. Chem.* **2012**, *51*, 7392−7403.
(12) Xiao, X.-S.; Kwong, W.-L.; Guan, X.; Yang, C.; Lu, W.; Che, C.-M. *Chem.—Eur. J.* **2013**, *19*, 9457−9462.
(13) Hashmi, A. S. K.; Braun, I.; Rudolph, M.; Rominger, F. *Organometallics* **2012**, *31*, 644−661.
(14) Ye, L.; Wang, Y.; Aue, D.; Zhang, L. *J. Am. Chem. Soc.* **2012**, *134*, 31−34.
(15) Hooper, T.; Green, M.; Russell, C. *Chem. Commun.* **2010**, *46*, 2313−2315.
(16) Hall, K. P.; Mingos, D. M. P. *Prog. Inorg. Chem.* **1984**, *32*, 237−325.
(17) Fernandez, E. J.; Monge, M. Gold nanomaterials. *Modern Supramolecular Gold Chemistry: Gold-Metal Interactions and Applications*; Wiley-VCH: Weinheim, 2008; pp 131−179.
(18) Jin, R. *Nanoscale* **2010**, *2*, 343−362.
(19) Lu, Y.; Chen, W. *Chem. Soc. Rev.* **2012**, *41*, 3594−3623.
(20) Tsukuda, T. *Bull. Chem. Soc. Jpn.* **2012**, *85*, 151−168.
(21) Maity, P.; Wakabayashi, T.; Ichikuni, N.; Tsunoyama, H.; Xie, S.; Yamauchi, M.; Tsukuda, T. *Chem. Commun.* **2012**, *48*, 6085−6087.
(22) Maity, P.; Tsunoyama, H.; Yamauchi, M.; Xie, S.; Tsukuda, T. *J. Am. Chem. Soc.* **2011**, *133*, 20123−20125.
(23) Kamei, Y.; Shichibu, Y.; Konishi, K. *Angew. Chem., Int. Ed.* **2011**, *50*, 7442−7445.
(24) Shichibu, Y.; Kamei, Y.; Konishi, K. *Chem. Commun.* **2012**, *48*, 7559−7561.
(25) Shichibu, Y.; Konishi, K. *Inorg. Chem.* **2013**, *52*, 6570−6575.
(26) Hargrove, A.; Zhong, Z.; Sessler, J.; Anslyn, E. *New J. Chem.* **2010**, *34*, 348−354.
(27) Hansmann, M. M.; Rominger, F.; Hashmi, A. S. K. *Chem. Sci.* **2013**, *4*, 1552−1559.
(28) Benitez, D.; Shapiro, N.; Tkatchouk, E.; Wang, Y.; Goddard, W.; Toste, F. *Nat. Chem.* **2009**, *1*, 482−486.